J. Min. Metall. Sect. B-Metall. 59 (2) (2023) 269 - 277

Journal of Mining and Metallurgy, Section B: Metallurgy

CORROSION OF A CHIMNEY LINER OPERATED FOR 130,000 HOURS

M. Gwoździk

Czestochowa University of Technology, Faculty of Production Engineering and Materials Technology, Department of Materials Engineering, Czestochowa, Poland

(Received 06 February 2023; Accepted 08 August 2023)

Abstract

The tests were carried out for a coal-fired boiler heating a single-family house with a floor area of 220 m^2. The tests concerned the chimney lining (structure and surface layer - produced oxides/deposits), hard coal (eco-pea coal) and furnace ash. The chimney liner was located in a chimney made of bricks joined with concrete. A chimney liner made of austenitic steel was tested. The chimney liner was operated for 130,000 hours. The chimney insert was studied on the insideand outside each cross-section. Coal with a grain size of 5–21 mm was analyzed. The bottom ash consisted of both loose ash and a mass of glassy sintered ash, the so-called slag. The thorough examinations of the examined materialsincludec: microscopic examinations with a VHX-7000 digital microscope and Jeol JSM-6610LV scanning electron microscopes. Chemical composition analysis by energy dispersive X-ray spectroscopy (EDS) in conjunction with the scanning electron microscopy (SEM) was performed. The surface topography (roughness) was measured with a VHX microscope using a Gaussian filter. Based on the tests, the following parameters were determined: arithmetic mean height, maximum height, height of the highest peak, depth of the lowest depression, root mean square height, skewness, kurtosis.

Keywords: *Chimney insert; Eco-pea coal; Austenitic steel*

1. Introduction

Air pollution is the most dangerous form of environmental pollution due to its direct impact on all living organisms, covering large areas and easy movement [1]. Particulate pollution is emitted not only from coal-fired power plants [2] and industrial facilities [2], but also from coal combustion in household furnaces [3]. Chimneys are made of, for example: reinforced concrete (RC) [4]. The literature data shows that as a result of the combustion of hard coal in household furnaces, the content of carbon chlorine has a large impact on the emission of the polychlorinated dibenzo p-dioxins and furans (PCDD/F) [3].Various gas pollutants from household furnaces are identified in the flue gases, including particulate matter (PM), polycyclic aromatic hydrocarbons (PAH), carbon monoxide (CO), and sulfur dioxide (SO_2) [5]. Hard coal is used by households, for example [6]. Hard coal is one of the main sources of anthropogenic mercury emissions into the atmosphere [6]. Mercury in coal coexists with sulfur, and in fly ash its content is correlated with the amount of unburnt coal [6]. Domestic heating boilers are not equipped with a flue gas cleaning system. They are also a source of low emission, which is the main cause of smog in cities and villages [6]. It should also be mentioned that some of the mercury emitted to the atmosphere is adsorbed on the surface of particulate matter, which intensifies the adverse effect of smog [6]. Hlawiczka et al. showed that in addition to mercury emitted to the atmosphere in gaseous form, a large part of mercury is present in the dust suspended in the flue and emitted to the air [7]. Coal ash also contains valuable elements such as: ferromagnetic fractions (> 3 wt.% Fe_2O_3) and SiO_x and MgO microspheres [8]. Currently, chimney liners for concrete or brick chimneys are increasingly used, which provide protective properties of the original external structure against chemicals, as well as thermal and corrosive environments. Chimney liners can be made of: glass fiber-reinforced polymer (GFRP) [9], fiberglass reinforced plastic (FRP) [10], titanium-steel composite [11], stainless steel [12], and carbon steel [13]. The composite (titanium-steel) liner system provides strength and rigidity to the carbon steel substrate, supporting a corrosion-resistant titanium sheet coating. However, in this type of structures, detachment of the titanium sheet from the carbon steel substrate was observed [11]. In the case of reinforced concrete and masonry chimneys, linings are used, for example, made of stainless steel [14], which has unique properties [15]. Chimney liners in

Corresponding author: monika.gwozdzik@pcz.pl

https://doi.org/10.2298/JMMB230206023G

these chimneys are used for safety reasons, because during the combustion of fuels, acidic water vapor is formed, which precipitates in the chimney, damaging, among others, the chimney, plaster, concrete. This acidic steam damages the layer of mortar between the bricks and destroys the internal structure of the chimney. Through the resulting gaps, carbon monoxide can escape into rooms, which can be fatal. Chimney liners should meet the following requirements [14]: (1) tightness, (2) chemical resistance to the harmful effects of chimney gases, (3) possibility of installation on complex (non-linear) chimneys, (4) resistance to fire and heat. The advantage of chimney inserts made of stainless steel pipes is their thin walls. As a result, they do not significantly reduce the effective cross-section of the chimney. However, due to the thinnes of the material, they are more prone to corrosion [14].

The purpose of this paper was to perform a material analysis of the operated chimney liner at its various heights. The tests carried out were aimed at determining the wear of both the surface and the structure of the chimney liner operating for a period of 130,000 hours.

2. Materials and metodology

The tests were carried out for a coal-fired boiler heating a single-family house with a floor area of 220m^2. The tests covered the chimney insert, hard coal (eco-pea coal), and furnace ash. The chimney liner was located in a chimney made of bricks joined with concrete. A chimney liner made of austenitic steel (of the tinware thickness 1 mm) was tested. The chimney liner was operated for 130,000 hours. The chimney insert was studied on the inner and outer side and the respective cross-section (Fig. 1). For this purpose, samples with dimensions of 10mm x 10mm were taken from the chimney insert. The specimens were made transversely to the material axis. The preparation of the metallographic specimen consisted of grinding and polishing. The chimney liner was tested at the height (counting from the bottom) of 4m, 8m and 12m. Coal with a grain size of 5–21mm was analyzed. The bottom ash consisted of both loose ash and a mass of glassy sintered ash, the so-called slag.

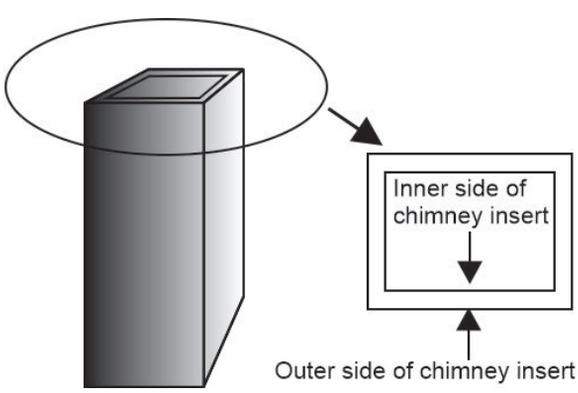

Figure 1. *Chimney insert - positions of the samples used for microstructure analyses*

Thorough examinations of the researches materials comprised: microscopic examinations using an digital microscope VHX-7000 and scanning electron microscopes Jeol JSM-6610LV. Analysis of the chemical composition using Energy dispersive X-ray spectroscopy (EDS) in conjunction with the scanning electron microscopy (SEM). The SEM operating parameters were as follows: voltage 20kV and working distance from 9 to 11mm. The measurement of the surface roughness was carried out with a VHX microscope using a Gaussian filter. On the basis of the tests carried out, the following parameters were determined:

S_a (arithmetic mean of height) - the average of the absolute values of the heights of each point of the specified area

$$S_a = \frac{1}{A}\iint_A |z(x,y)|\,dxdy \quad [16, 17]$$

S_z (maximum height) - the sum of the height of the highest elevation and the depth of the lowest depression in the area

$$S_z = S_p + S_v \quad [16]$$

S_p (height of the highest hill) - this is the height of the highest point of the specified area

$$S_p = \max z(x,y)$$

S_v (depth of the lowest depression) [18] – this is the absolute value of the depth of the lowest point of a specific area

$$S_v = |\min z(x,y)|$$

S_q (rms height) – the rms height at each point in the area. This is equivalent to the standard deviation of height

$$S_q = \sqrt{\frac{1}{A}\iint_A z^2(x,y)\,dxdy} \quad [17]$$

S_{sk} (skewness) – this is the third-order mean calculated on the basis of the cube of the root mean square S_q. Indicates asymmetrical height distribution centered on the reference surface.

$$S_{sk} = \frac{1}{S_q^3}\left[\frac{1}{A}\iint_A z^3(x,y)\,dxdy\right] \quad [16]$$

S_{ku} (kurtosis) – it is the fourth power mean of the height calculated on the basis of the fourth power of the root mean square S_q. Indicates a flattening of the height distribution.

$$S_{ku} = \frac{1}{S_q^4}\left[\frac{1}{A}\iint_A z^4(x,y)\,dxdy\right] \quad [16]$$

3. Results and discussion

The hard coal used for combustion contained in its chemical composition, apart from organic substances that form the basic composition of coal, such as: carbon, hydrogen, oxygen, nitrogen, sulfur, also impurities in the form of ash based on the following elements: Al, Si, K, Ca, Fe. These elements are related to in oxides such as: Al_2O_3, Fe_2O_3, SiO_2, CaO, K_2O. According to the literature [19], the main elements of carbon are: C, H, O, N and S, where the relative proportion of C increases as the magma intrusion distance increases, whereas the residual elements, such as H, O, N and S, show an opposite tendency [20]. The sulphide minerals found in coal are mainly pyrite [21]. A lower share of SiO_2 oxides in coal compared to Al_2O_3 was observed by Ikeh et al. at paper [21]. An example image of coal topography used for combustion is shown in Figure 2.

The obtained test results of the chimney liner showed that, depending on its location, there is a differentiated degradation. As shown in Figure 3, the lowest degree of degradation is characterized by the chimney liner closest to the inlet to the furnace. Going up, i.e. at the height of 8 meters from the inlet, the degradation is already progressing significantly. Directly at the outlet from the chimney, i.e. at a height of 12 meters from the ground, the complete exploitation of the tested chimney liner is visible for the most part.

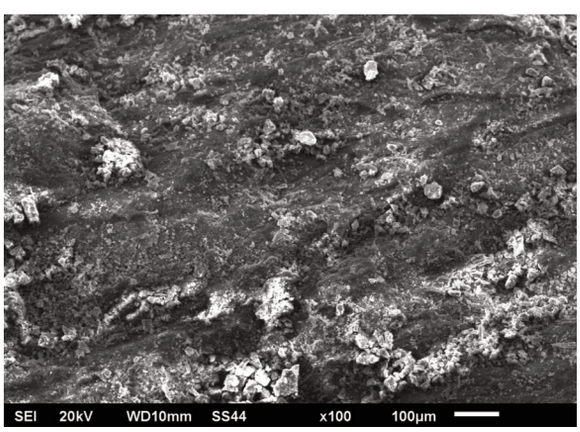

Figure 2. *Carbon surface*

A varied structure of the chimney liner was observed depending on its location in the chimney. Near the inlet to the furnace, polygonal austenite grains with formed twins and carbide precipitates are observed (Fig. 4a). The addition of 8% nickel in steel with a concentration of 18% chromium provides corrosion-resistant steels with a durable austenitic structure. Austenitic steels with the fcc crystallographic structure (wall centered) are used as materials for storage and transport in cryogenic conditions, e.g. due to their high corrosion resistance [22]. As it moves away from the inlet, a progressive degradation of the structure is observed. The twins are gradually being destroyed. Craters can be seen forming. In addition, there are visible empty places after carbide precipitations (Fig. 4b). The formation of craters on this type of steel was also observed by Tian et al. [23]. They researches investigated the effect of stress on the microstructure evolution of 316L SS and 304 SS steels subjected to cavitation erosion and cavitation erosion-corrosion. Figure 4c, on the other hand, shows the structure of the tested chimney liner directly from the side of the flue gas outlet. In places, complete degradation of the structure is visible. The chimney liner in this area was locally damaged over the entire thickness of the sheet metal wall.

The observations of the outer and inner (Fig. 5) walls of the chimney insert showed a varied amount of deposits, not only depending on the side of their location, but also on the height of the insert. The microscopic observations show that the inner side of the chimney liner was degraded regardless of where the sample was taken. In all three cases, the surface of the top layer was damaged (Fig. 5). A layer of sediments and progressing corrosion pits are visible. The obtained results indicate that the sample taken directly at the chimney outlet is characterized by the highest degree of degradation. Only a small amount of sediment can be observed on this sample, the rest of the area is just pits. In each of the analyzed cases, the deposits formed show numerous

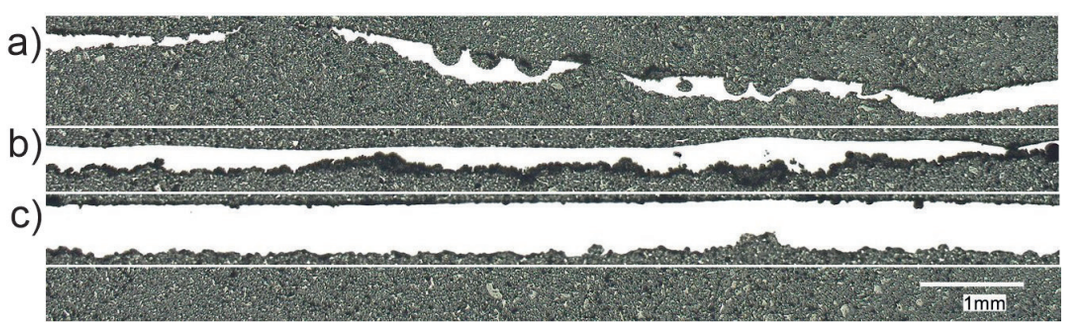

Figure 3. *Differentiated degradation of the chimney liner: (a) 12m from the ground, (b) 8m from the ground, (c) 4m from the ground*

cracks (Fig. 6), which would indicate a significant post-mining degradation of the above-mentioned structure.

A different situation was observed for the external side. From this side, no corrosion pits were observed on the surface at a distance of 4 meters from the ground (Fig. 7a). The pits appear only in the upper part of the chimney liner (Fig. 7b, c). In Fig. 7b, occasional pits are visible. What is important, however, is that at 8 meters in the outer layer of sediment, cracks begin to appear. Observations of the external side of the chimney liner directly from the flue gas outlet have already shown quite numerous presence of pits. In Fig. 7c, from the left side, a pit extending deep into the structure is visible. The irregular nature of the corrosion damage on the surface indicates pitting/crevice corrosion. A similar character of corrosion was observed in [24]. According to the literature [25] austenitic stainless steels type 316, 317 and 904L are subject to pitting and crevice corrosion. Moreover, a similar course of cracks was observed in [24]. SEM micrographs of the chimney liner surface at lower magnification show several depressions, and at higher magnification show small cracks in a wide and shallow pit. The condensation of harmful combustion products takes place in the upper part of the chimney and thus the chimney liner. In the lower parts of the chimney there are high temperatures, i.e. higher than the dew point of the oxidizing gases. As a result, the gases accumulate in the upper parts of the chimney, where the temperature drops below the dew point.In these parts, saturated condensate corrodes the chimney by accumulating soot on the walls of the chimney. The accumulation of soot, in turn, may reduce the cross-section of the chimney, which in turn may lead to the phenomenon of saturation of the lower parts of the chimney with condensate [24].

The chemical composition of the deposits formed on both the outer and inner side of the wall of the chimney insert was characterized by the occurrence of, among others, elements such as: Fe, C, O, Si, S, Cl, Cr, and Cu. In addition, Na, Mg, Al, K, Ca, Mn, and Zn were also not observed in all cases, as shown in Table 1. This would indicate the presence of such compounds as: SiO_2, Al_2O_3, Fe_2O_3, CaO, K_2O, MnO, and MgO. The occurrence of similar compounds was observed in [6]. The authors of [24] showed that the spectrum rich in sulfur and carbon indicates the presence of soot, ash, and acidic compounds rich in sulfur. A deposit corresponding to a spectrum consisting mainly of calcium, oxygen, and sulfur indicates the possibility of

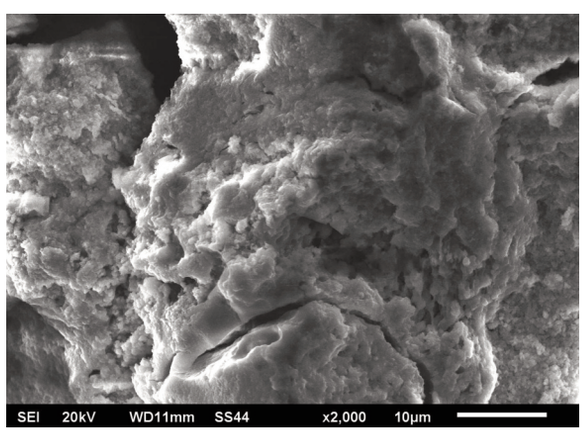

Figure 6. *Cracks in the deposits on the inside wall of the chimney liner*

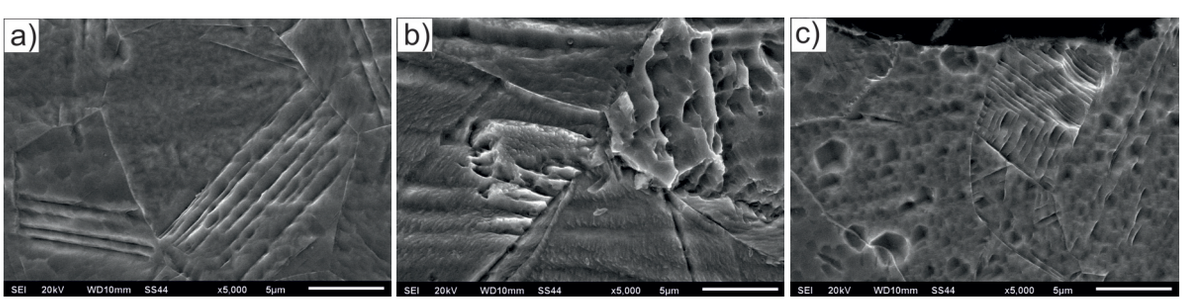

Figure 4. *Chimney liner structure: (a) 4m from the ground, (b) 8m from the ground, (c) 12m from the ground*

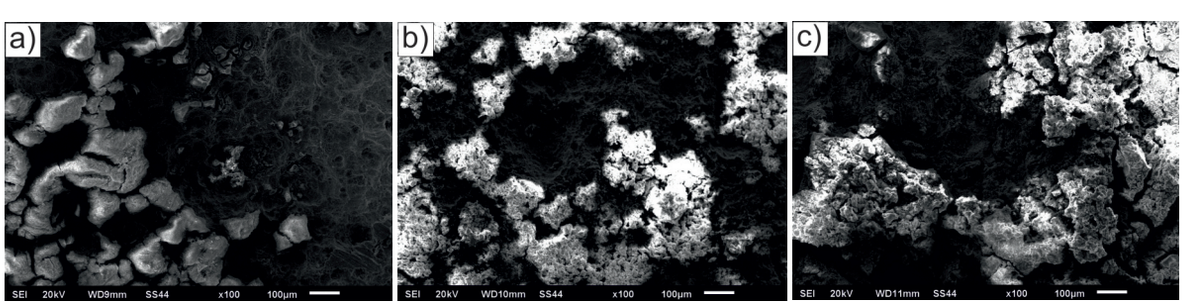

Figure 5. *The inner side of the chimney liner wall: (a) 12m from the ground, (b) 8m from the ground, (c) 4m from the ground*

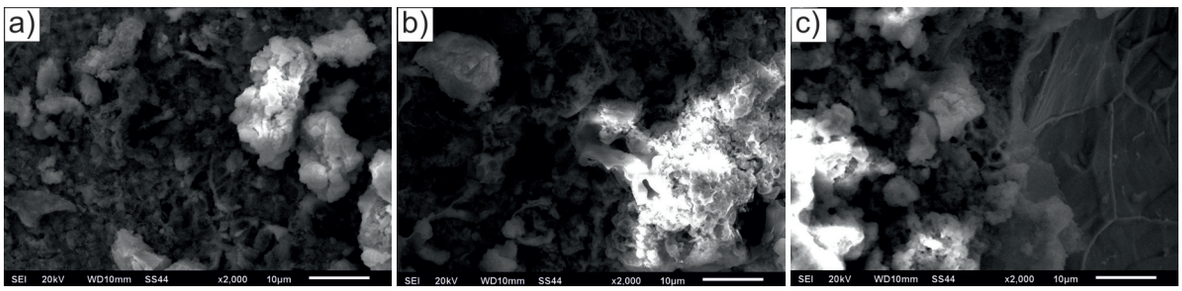

Figure 7. *The outer side of the chimney liner wall: (a) 4m from the ground, (b) 8m from the ground, (c) 12m from the ground*

the presence of the compound $CaSO_4$. In turn, the precipitate corresponding to the spectrum rich in silicon and oxygen may be silica. In addition, the researchers also observed a chlorine peak indicating the presence of chloride ions in the condensates. Chlorides, fluorides, and other impurities can worsen corrosion [25]. The presence of other elements in the sediments, such as magnesium or potassium, indicates that flue gas condensation takes place in conjunction with rainwater or atmospheric moisture over a long period of time. In addition, the researchers found that the condensate was strongly acidic and consisted mainly of H_2SO_4 [24]. Corrosion on the chimney liner usually occurs in the low-temperature part of the combustion equipment. It is usually caused by the acidic fumes of the combustion gases that condense on exposed surfaces, causing damage to the material. This occurs when the ambient temperature drops below the dew point, causing water, acid or other liquid to condense. In boiler technology, the "acid dew point" means the dew point temperature of H_2SO_4, because it is the highest temperature at which acid condensation occurs [24]. Also, after flue gas desulfurization, the flue gas in the chimney contains a certain amount of acidic components [25], e.g. SO_2 with high humidity and temperature around 50°C. Flue gases containing SO_2 easily condense when the ambient temperature drops below the dew point, forming highly corrosive electrolytes, the main component of which is sulfuric acid [26]. Oil and natural gas contain a lot of sulfur, and coal contains a lot of nitrogen. The water vapor from the flue gas reacts with carbon dioxide, sulfur dioxide and sulfur trioxide. The result is H_2CO_3, H_2SO_4 and H_2SO_3. Alkali silicates and acids become salts, which causes corrosion in chimneys [14]. Corrosion is the greatest threat to chimney liners [14]. According to literature data [24], austenitic corrosion-resistant steels type 316 or 317 show higher corrosion resistance than 304 steel, reaching up to 25% H_2SO_4. According to the literature, corrosion damage occurs in the cladding and/or body of the structure, whether it is non-alloy steel, corrosion-resistant steel, nickel alloy or concrete [24]. This corrosion is mainly located on the inner surface near the outer flanges or ladder fasteners due to local cooling effects [24].

Sediments separated from the inside were characterized in terms of morphology. Three different types of these deposits were observed. The first one has the character of fine, strongly compact structures (Fig. 8a). The second type is an irregular structure. Settlements of this nature form agglomerations in places resembling the so-called honeycomb (Fig. 8b). The third type of sediment is characterized by a completely different structure. In this case, fine sphere-like deposits are placed under a compact smooth surface. To a large extent, this surface is cracked (Fig. 8c). The analysis of the chemical composition of isolated sediments (Table 2) showed that the first type is characterized by the presence of such elements as O, Fe, Cr, C, Cl, S, and Ni. In the second type, the presence of silicon and potassium was additionally found. The third type, in addition to the above-mentioned elements, additionally contained calcium and manganese, but no carbon was found in its composition.

The obtained roughness measurement results (Fig. 9, Table 3) for the inner side of the chimney liner showed the lowest value of the parameter S_a=10.13μm for the sample placed closest to the furnace. The surface development directly at the outlet was much greater with the arithmetic mean height being 23.32μm. Roughness measurements are very helpful in determining the roughness of deposits/oxides [27]. A similar increase was observed for the S_z parameter, where it was 91.15μm, 148.59μm, and 160.66μm, respectively. For the outside of the chimney liner, the arithmetic mean height was 1.96μm at a height of four meters. However, a significant increase of this parameter to 31.25μm was observed directly at the chimney outlet. Such high roughness is due to the fact that the layer of sediments has largely fallen away in the places where the pits are located. The value of the S_{sk} parameter is closest to zero for the sample that was taken from a height of eight meters both from the inside and outside of the chimney liner, which would mean that the height distribution is symmetrical to the reference plane. In other cases, the height distribution is slanted up or down relative to the reference plane. The obtained measurement results indicate that for the sample from the inside at a height of 8m, the distribution of the height of the surface irregularities is

Table 1. *Chemical composition of sediments*

	Meters from the ground	Chemical composition / weight %							
		C	O	Na	Mg	Al	Si	S	Cl
The inner side of the wall of the chimney insert	4	3.50	20.90	-	-	-	0.15	2.61	2.48
	8	4.94	13.73	0.65	-	0.16	0.22	2.39	3.57
	12	11.95	34.23	-	-	0.29	0.28	4.00	3.44
		K	Ca	Cr	Mn	Fe	Ni	Cu	Zn
	4	0.16	-	14.02	0.81	48.43	6.28	0.66	-
	8	-	0.16	16.73	1.32	46.57	5.99	0.49	3.08
	12	0.58	-	13.87	-	26.66	2.59	2.12	-
The outer side of the wall of the chimney insert		C	O	Na	Mg	Al	Si	S	Cl
	4	7.13	29.43	0.84	0.20	2.34	0.44	3.67	6.67
	8	18.75	22.80	0.27	0.48	0.89	0.45	1.35	2.46
	12	16.06	24.97	0.52	0.32	1.30	0.49	3.14	3.01
		K	Ca	Cr	Mn	Fe	Ni	Cu	Zn
	4	0.89	0.68	8.68	0.36	33.35	4.67	0.62	-
	8	0.18	0.48	9.98	0.51	36.96	4.06	0.37	-
	12	-	0.20	8.46	-	34.35	4.36	0.54	2.28

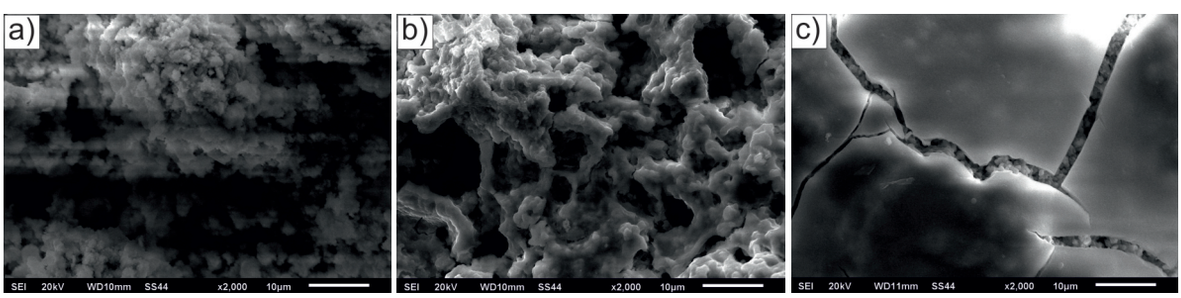

Figure 8. *Isolated deposits: (a) I type, (b) II type, (c) III type*

Table 2. *Chemical composition of isolated sediments*

	Chemical composition / weight %										
	C	O	Si	S	Cl	K	Cr	Fe	Ni	Ca	Mn
I type	9.41	39.57	-	1.32	8.42	-	9.78	30.31	1.19	-	-
II type	8.74	40.21	0.85	6.52	7.15	0.46	6.87	26.89	2.30	-	-
III type	-	40.37	1.20	7.60	9.19	0.54	8.39	29.37	2.75	0.26	0.33

the closest to the normal distribution, which is indicated by the S_{ku} parameter.

The test results obtained from the bottom ash showed (Fig. 10, Table 4) that it is characterized by a significantly lower sulfur content compared to the sludge from the chimney liner. This statement was confirmed in [6]. Researchers found that boiler deposits are characterized by a much higher sulfur content compared to furnace ash [6]. As the tests showed, no sulfur was detected in the burnt coal (Table 5). The structure of burnt coal is shown in Figure 11. Observations of coal fly ash using a scanning electron microscope were also carried out by Yu et al. [28]. As a result of coal combustion, a high ash content is obtained [29]. According to the literature, samples taken from coal were characterized by high sulfur content, 2.16% and 2.76%, respectively [6]. The ash samples were also characterized by a high content of sulfur from 2.24 to 3.11% and a relatively high content of unburnt carbon from 21.6 to 27.8% (on a dry weight basis) [6]. Settling on the walls of the chimney, soot formed an effective layer of adsorbent. In addition, it was found that other ecotoxic elements are also adsorbed in large amounts on the surface of chimney soot, e.g. As, Pb, Cu, Zn, Ni, Cr, which are commonly present in hard coal [6].

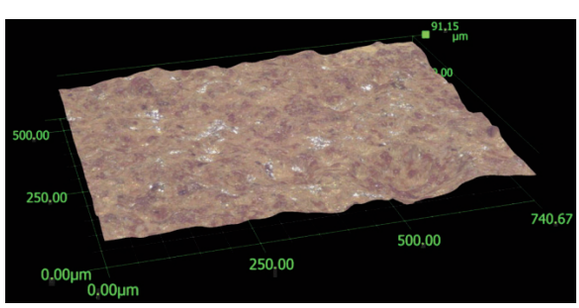

Figure 9. *An example 3d image - the inside of the wall of the chimney insert*

Table 3. *Roughness measurements*

	The inner side of the wall of the chimney insert			The outer side of the wall of the chimney insert		
	Meters from the ground					
	4	8	12	4	8	12
S_a / µm	10.13±0.61	19.28±1.11	23.32±1.52	1.96±0.32	7.69±0.27	31.25±1.93
S_z / µm	91.15±4.87	148.59±7.52	160.66±7.87	47.56±1.99	65.17±4.02	214.97±9.04
S_q / µm	13.52±0.98	24.49±1.63	29.47±1.78	3.48±0.08	9.32±0.34	43.98±2.65
S_{sk}/ -	-1.11±0.09	0.11±0.01	-0.25±0.02	3.98±0.21	-0.16±0.02	1.65±0.04
S_{ku}/ -	5.25±0.56	2.87±0.05	2.72±0.06	29.46±2.03	2.47±0.07	5.46±0.11
S_p / µm	32.73±2.08	68.65±3.04	78.95±2.54	33.02±1.02	40.51±3.21	136.8±4.32
S_v / µm	58.43±2.98	79.94±3.33	81.7±3.77	14.53±0.53	24.66±2.12	78.17±4.43

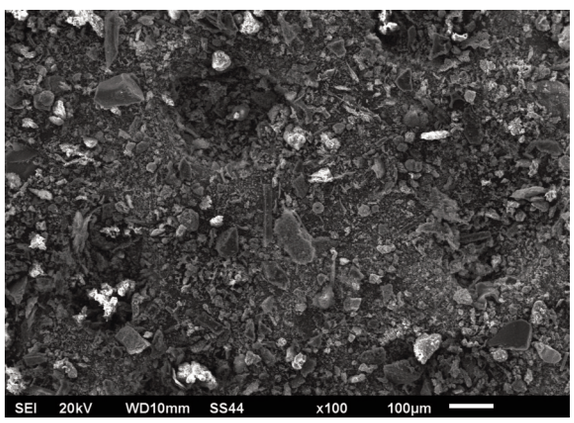

Figure 10. *Combustion ash*

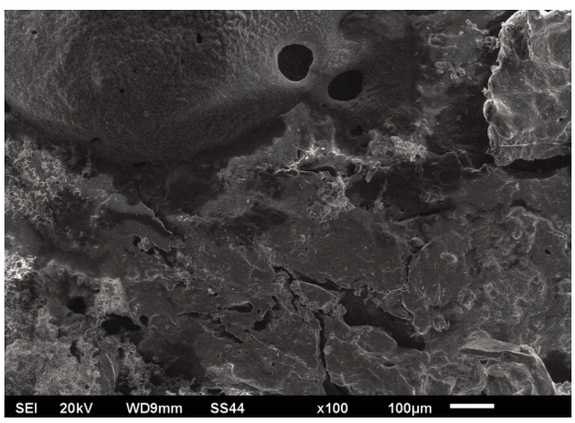

Figure 11. *Burned coal*

Table 4. *Chemical composition of combustion ash*

Chemical composition / weight %												
C	O	Na	Mg	Al	Si	P	S	Cl	K	Ca	Ti	Fe
43.12	33.69	0.93	0.53	6.09	5.28	0.17	0.86	2.89	0.34	2.11	0.58	3.41

Table 5. *Chemical composition of burnt coal*

Chemical composition / weight %								
O	Na	Mg	Al	Si	K	Ca	Ti	Fe
58.92	1.22	3.8	11.7	14.82	1.31	1.34	0.35	6.54

4. Conclusions

1. The structure of the chimney liner changed depending on its location. Directly near the chimney outlet, the structure is completely degraded. The chimney liner in this place was completely destroyed over the entire cross-section.
2. The inner side of the chimney liner has degraded regardless of where the material was taken.
3. The outer side of the chimney liner shows significant degradation only directly from the chimney outlet.

Author contributions

Writing-original draft, investigation, conceptualization, editing: Monika Gwoździk

Data availability

The data used to support the findings of this study are available from the corresponding author upon request.

Conflict of interest

The author declare that they have no known

competing financial interests or personal relationships that could have appeared to influence the work reported in this paper.

References

[1] D. Proszak, S. Rabczak, E. Rybak-Wilusz, Ecological and financial effects of coal-fired boiler replacement with alternative fuels, Journal of Ecological Engineering, 21 (1) (2020) 1-7. https://doi.org/10.12911/22998993/113638

[2] D. Shin, Y. Kim, K.J. Hong, G. Lee, I. Park, H.J. Kim, Y.J. Kim, B. Han, J. Hwang, Measurement and analysis of PM10 and PM2.5 from chimneys of coal-fired power plants using a light scattering method, Aerosol and Air Quality Research, 22 (2) (2022) 210378. https://doi.org/10.4209/aaqr.210378

[3] B. Paradiz, P. Dilara, G. Umlauf, I. Bajsic, V. Butala, Dioxin emissions from coal combustion in domestic stove: formation in the chimney and coal chlorine content influence, Thermal Science, 19 (1) (2015) 295-304. https://doi.org/10.2298/TSCI140113079P

[4] Y.S. Cheng, K.S. Dai, Y.Z. Liu, H. Yang, M.R. Sun, Z.H. Huang, A. Camara, Y.X. Yin, A method for along-wind vibration control of chimneys by tuning liners, Engineering Structures, 252 (2022) 113561. https://doi.org/10.1016/j.engstruct.2021.113561

[5] C.T. Liu, C.L. Zhang, Y.J. Mu, J.F. Liu, Y.Y. Zhang, Emission of volatile organic compounds from domestic coal stove with the actual alternation of flaming and smoldering combustion processes, Environmental Pollution, 221 (2017) 385-391. https://doi.org/10.1016/j.envpol.2016.11.089

[6] T. Dziok, P. Grzywacz, P. Bochenek, Assessment of mercury emissions into the atmosphere from the combustion of hard coal in a home heating boiler, Environmental Science and Pollution Research, 26 (22) (2019) 22254-22263. https://doi.org/10.1007/s11356-019-05432-3

[7] S. Hlawiczka, K. Kubica, U. Zielonka, Partitioning factor of mercury during coal combustion in low capacity domestic heating units, Science of the Total Environment, 312 (1-3) (2003) 261-265. https://doi.org/10.1016/S0048-9697(03)00252-3

[8] Sh.R. Malikov, V.P. Pikul, N.M. Mukhamedshina, V.N. Sandalov, S. Kudiratov, E.M. Ibragimova,.Content and distribution of transition metals and rare earth elements in magnetically and mechanically separated brown coal ash, Journal of Magnetics, 18 (3) (2013) 365-369. https://doi.org/10.4283/JMAG.2013.18.3.365

[9] S. Cheng, P. Feng, X.M. Meng, Z.Y. Li, J.K. Du, Compression behavior of large-scaled cylindrical GFRP chimney liner segments, Composite structures 232 (2020) 111543. https://doi.org/10.1016/j.compstruct.2019.111543

[10] S.D. Li, J.D. Eisenman, D. Mikulec, Prediction of ovalling frequency for FRP chimney liners with circumferential stiffeners, Journal of Thermoplastic Composite Materials, 25 (4) (2012) 439-451. https://doi.org/10.1177/0892705711411342

[11] R.H.R. Tide, M.H. Darr, Proc. 2nd International Conference on Thin-Walled Structures 02-04.12.1998, Signapore, Signapore, 1998, p.271-278.

[12] H. Schmidt, U. Kocabiyik, Proc. International Conference on Steel Structures of the 2000's, 11-13.09.2000, Istambul, Turkey, 2000, p.257-262.

[13] L.C. Vangansbeke, D.C. Pattison, Proc. 59th Annual Meeting of the American-Power-Conference on Competitiveness Through Technology and Cooperation,1997, Chicago, USA, 1997, p.315-320.

[14] Z. Kererekes, E. Lubloy, B. Elek, A. Restas, Standard fire testing of chimney linings from composite materials, Journal of Building Engineering, 19 (2018) 530-538. https://doi.org/ 10.1016/j.jobe.2018.05.030

[15] J. Iwaszko, K. Kudła,Surface modification of ZrO2-10 wt. % CaO plasma sprayed coating, Bulletin of the Polish Academy of Sciences - Technical Sciences, 64 (4) (2016) 937-942. https://doi.org/10.1515/bpasts-2016-0102

[16] P. Turek, G. Budzik, J. Sęp, M. Oleksy, J. Józwik, Ł. Przeszłowski, A. Paszkiewicz, Ł. Kochmański, D. Żelechowski, An analysis of the casting polymer mold wear manufactured using PolyJet method based on the measurement of the surface topography, Polymers, 12 (2020) 3029, https://doi.org/10.3390/polym12123029

[17] J. Xiong, L. Wan, Y.N. Qian, S. Sun, D. Li, S.J. Wu, A new strategy for improving the surface quality of Ti6Al4V machined by abrasive water jet: reverse cutting with variable standoff distances, The International Journal of Advanced Manufacturing Technology, 120 (2022) 5339-5350. https://doi.org/10.1007/s00170-022-09091-6

[18] Z. Zhu, S. Lou, C. Majewski, Characterisation and correlation of areal surface texture with processing parameters and porosity of High Speed Sintered parts, Additive Manufacturing, 36 (2020) 101402. https://doi.org/10.1016/j.addma.2020.101402

[19] Z.T. Zhang, W.F. Li, J. Zhan, The effect of coal ratio on the high-lead slag reduction process, Journal of Mining and Metallurgy Section B-Metallurgy, 54 (2) B (2018) 179-184. https://doi.org/10.2298/JMMB171227006Z

[20] S.B. Feng, Q. Wei, X.Q. Li, Chemical composition variations of altered and unaffected coals from the Huaibei Coalfield, China: Implications for Maturity, Energies, 14 (2021) 3028. https://doi.org/10.3390/en14113028

[21] T.J. Ikeh, BL. Sun, C. Liu,Y.X. Liu,Y.L. Kong, X.Y. Pan, Modes of occurrence and enrichment of trace elements in coal from the Anjialing Mine, Pingshuo Mining District, Ningwu Coalfield, Shanxi Province, China, Minerals, 12 (2022) 1082. https://doi.org/10.3390/min12091082

[22] J.C. Lee, Y. Noh, N.S. Kim, K.B. Park, H. Kim, H.H. Cho, H.K. Park, T.S. Jun, C.S. Park, Effect of texture and temperature on strain-induced martensitic transformation in 304 austenitic stainless steel, Steel Research International, Early Acces (2022) 2200243. https://doi.org/10.1002/srin.202200243

[23] Y. Tian, H. Zhao, R. Yang, X.M. Liu, X.Y. Chen, J.H. Qin, A. McDonald, H. Li, In-situ SEM investigation on stress-induced microstructure evolution of austenitic stainless steels subjected to cavitation erosion and cavitation erosion-corrosion, Materials & Design, 213 (2022) 110314. https://doi.org/10.1016/j.matdes.2021.110314

[24] K. Chandra, V. Kain, G.K. Dey, Accelerated corrosion of a boiler chimney: causes and preventive steps, Journal of Failure Analysis and Prevention, 11 (5) (2011) 466-472. https://doi.org/10.1007/s11668-011-9474-8

[25] Z.Y. Cui, L.W. Wang, H.T. Ni, W.K. Hao, C. Man, S.S.

Chen, X. Wang, Z.Y. Liu, X.G. Li, Influence of temperature on the electrochemical and passivation behavior of 2507 super duplex stainless steel in simulated desulfurized flue gas condensates, Corrosion Science, 118 (2017) 31-48. https://doi.org/10.1016/j.corsci.2017.01.016

[26] F. Ge, L.W. Wang, Y.P. Dou, J.Y. Wei, L.J. Cheng, X. Wang, Z.Y. Cui. Elucidating the passivation kinetics and surface film chemistry of 254SMO stainless steel for chimney construction in simulated desulfurized flue gas condensates, Construction and Building Materials, 285 (2021) 122905. https://doi.org/10.1016/j.conbuildmat.2021.122905

[27] M. Gwoździk, S. Kulesza, M. Bramowicz, Proc. 26th International Conference on Metallurgy and Materials, 24-26.05.2017, Brno, Czech Republic, 2017, p.789-794.

[28] Q.C. Yu , Y. Deng, S.B. Yin, Z.Y. Li, Thermal process for magnesium production with Al.-Si-Fe from coal fly ash: thermodynamics and experimental investigation, Journal of Mining and Metallurgy Section B-Metallurgy, 57 (3) (2021) 421-430. https://doi.org/10.2298/JMMB210118038Y

[29] F.A. Atiku, E.J.S. Mitchell, A.R. Lea-Langton, J.M. Jones, A. Williams, K.D. Bartle, The impact of fuel properties on the composition of soot produced by the combustion of residential solid fuels in a domestic stove, Fuel Processing Technology, 151 (2016) 117-125. https://doi.org/10.1016/j.fuproc.2016.05.032

KOROZIJA OBLOGE DIMNJAKA POSLE 130000 SATI RADA

M. Gwoździk

Tehnološki univerzitet u Čestohovi, Fakultet za proizvodno mašinstvo i tehnologiju materijala, Odsek za inženjerstvo materijala, Čestohova, Poljska

Apstrakt

Ispitivanja su sprovedena na kotlu na ugalj koji greje porodičnu kuću površine 220 m^2. Ispitivanja su se odnosila na oblogu dimnjaka (struktura i površinski sloj – proizvedeni oksidi/naslage), kameni ugalj (eko-grašak ugalj) i pepeo iz peći. Obloga dimnjaka se nalazila u dimnjaku od cigle spojenih sa betonom. Ispitana je obloga dimnjaka od austenitnog čelika. Dimnjak je radio 130000 sati. Obloga dimnjaka je ispitana sa unutrašnje i spoljašnje strane svakog poprečnog preseka. Analiziran je ugalj veličine zrna 50–210 mm. Donji pepeo se sastojao od rastresitog pepela i mase staklastog sinterovanog pepela zvanog šljaka. Temeljna ispitivanja testiranih materijala obuhvatala su: mikroskopska ispitivanja digitalnim mikroskopom VHKS-7000 i skenirajucim elektronskim mikroskopom Jeol JSM-6610LV. Analiza hemijskog sastava energetsko disperzivnom rendgenskom spektroskopijom (EDS) u kombinaciji sa skenirajućom elektronskom mikroskopijom (SEM) je izvršena. Topografija (hrapavost) površine je merena VHKS mikroskopom korišćenjem Gausovog filtera. Na osnovu ispitivanja utvrđeni su sledeći parametri: aritmetička srednja visina, maksimalna visina, visina najvišeg vrha, dubina najniže depresije, srednja kvadratna visina, iskrivljenost, kurtoza.

Ključne reči: *Obloga dimnjaka; Eko-grašak ugalj; Austenitni čelik*